Joint Special Interest Group meeting between euspen and ASPE
Advancing Precision in Additive Manufacturing
KU Leuven, Belgium, September 2023
www.euspen.eu

Manufacture of designed porosities using pulsed laser powder bed fusion

Aakil Raj Lalwani[1], Mohamad Bayat[1], David Bue Pedersen[1], Jesper H Hattel[1], Venkata K Nadimpalli[1]

[1]*Technical University of Denmark, Institute of Civil and Mechanical Engineering, Denmark*

arala@dtu.dk

Abstract
Laser powder bed fusion is used to build products for medical, aerospace, and automotive industries due to the capability of this process in manufacturing complex geometries. An experimental study is carried out to characterize micro-lattices manufactured using a modulated pulsed wave (PW) laser as opposed to conventional laser powder bed fusion processes that use a continuous wave (CW) laser. PW promises smaller grains (as compared to CW) in the microstructure of parts, improved strength, and a more uniform melt pool with higher control of energy deposition which provides improved feature accuracy as well as surface topography. Lattice structures are particularly advantageous for lightweight components by designing void spaces. Micro-features can be efficiently characterized under a microscope but at the expense of a component. The designed porosities are characterized by using X-ray computed tomography and validated.

Laser powder bed fusion, metal additive manufacturing, lattice structures, x-ray computed tomography, pulsed laser.

1. Introduction

Additive Manufacturing (AM) is capable of manufacturing objects with intricate and complex geometries owing to its layer-wise manufacturing process. Laser powder bed fusion (L-PBF) is an AM process which uses a laser to selectively melt or fuse powder material in layers to build an object. Owing to the nature of the process, L-PBF makes efficient use of raw materials and allows for a high degree of design variance between parts manufactured simultaneously. Conventional subtractive manufacturing processes are wasteful and don't allow for a high degree of complexity. It is due to these advantages that AM processes are being adopted as one of the methods for manufacturing orthoses and prostheses [1] and hence the same can be made possible for biomedical implants.

Commonly, continuous-wave lasers are used in laser powder bed fusion. Pulsed wave, as the name suggests, modulates the laser input allowing for the processability of a wider range of materials. Pulsing of the laser provides control over energy deposition into the material, hence producing less porous and more precise parts [2]. Therefore, a pulsed L-PBF could potentially produce parts with the type of precision that is required for orthopaedic implants. The bones in the human body are load-bearing structures as well as lightweight porous structures [3]. To replicate something like the human bone parts will have to be designed with porosities and manufactured with high precision. In literature, it has been seen that inherently porous metallic implants made by AM facilitate good tissue ingrowth [4] and hence optimally designed porosities can improve acceptance of and fit of the implant. However, parts manufactured using L-PBF do not have optimal part quality and hence need to have some sort of post-treatment to achieve a more desirable part quality [5]. Metal L-PBF components with overhanging features are limited by the angle (45 degrees with respect to horizontal) of the overhanging face due to dross formation; which is a consequence of the nature of the process and the high thermal conductivity of metals [6]. Hence, they need to be manufactured using support structures which need to be machined out since they are not part of the designed geometry [7]. It is impossible to machine out material from the interior of an object hence manufacture of designed internal porosities is one of the main focuses of this work.

In this work, solid objects with designed porosities were made without support structures by using pulsed laser powder bed fusion. A method to characterize the geometric structures and porosities was established.

2. Methodology

2.1. Design

A benchmark (see Figure 1) was designed to quantify the system's capabilities to manufacture micro-features precisely. The benchmark part consists of four cuboidal volumes consisting of porosities designed by replacing the bulk with a body-centred cubic lattice. The dimensions of each of the designed porosities is listed in Table 1. Characterization and analysis of the designed porosities will be the focus of this work.

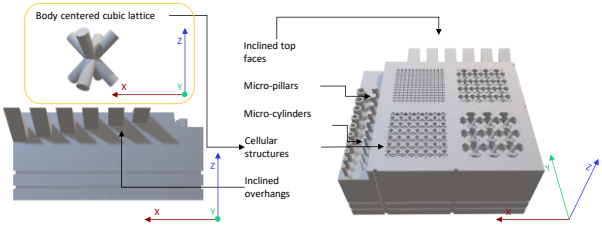

Figure 1 Design of benchmark part

Table 1 Dimensions for designed porosities

Bounding box of benchmark	Lattice strut diameter (mm)	Lattice unit cell side (mm)
26 * 26 * 12 mm^3	0.15	0.60
Bounding box of designed porosity	0.30	1.20
	0.45	1.80
8 * 8 * 8 mm^3	0.60	2.40

2.2. Materials and processing

Manufacturing was carried out on an in-house built L-PBF equipment, BAXTER [8]. The pre-processing of the CAD before printing and control was also done on an in-house developed Python-based software, AM Lab software. The software is just an interface, the control is possible due to the machine's in-house developed unified systems controller, i.e. GLAMS-Galvanometer Laser Additive Manufacturing System [9]. One of its unique features is that it enables the operation of the laser in continuous mode and pulsed mode. The pulsed laser output is controlled by setting the duty cycle and frequency. The laser on duration in pulsed mode is given by Equation (1)

$$\text{Laser } ON \text{ duration } (L_{on}) = c * \frac{d}{100}(sec) \quad (1)$$

Where, *c* is the period of one cycle in seconds (s) i.e. inverse of the frequency *f* in Hz, and *d* is the duty cycle in percentage (%).

BAXTER consists of a 250W SPI fiber laser and the optical setup consists of a beam expander and collimator in the laser delivery path to the galvanometer scanner from Scanlabs AG. The scanning system has an F-theta lens mounted on it and a protective window in front that separates it from the build chamber. The measured laser spot size in the mentioned arrangement was 70-80µm.

The material used for this work was stainless steel 316L purchased from Höganäs AB, having particle sizes ranging from 20-53µm. The common process parameters for the parts manufactured are listed in Table 2. The benchmark parts were manufactured at different duty cycles for the frequency 1000 Hz. The duty cycles used were 70%, 80%, 90%, and 100%. All the parts were manufactured in a Nitrogen rich atmosphere. Since previous research shows that it facilitates a good cellular structure and better hardness profile as compared to Argon gas, due to a more stabilised and homogenous distribution in the manufactured samples [10].

Table 2 Common process parameters for all manufactured parts

Hatch spacing: 80 µm	Laser power: 200 W	Layer thickness: 40 µm
Scan pattern: parallel lines	Scan speed: 400 mm/s	
Contours: off	Scan rotation (successive layers): 67°	

The benchmark parts were manufactured in 2 batches, such that each build job consisted of only 2 parts each (see Figure 2). Firstly, reduction of the inter-layer cooling time (duration for which the laser is off) for each individual part. Secondly, to arrange parts on the build plate to have optimal crossflow over it, ensuring that maximum spatter is taken away. As a benefit of this, the parts could be oriented in a way that the recoater will have a minimal influence on built-up edges (if any) during the powder distribution cycle.

2.3. Post-processing

After the completion of the manufacturing process, the loose powder was cleaned away manually, and benchmark parts were cut off the build plate with a band saw manually. The designed porosities were cut away from the benchmark design bulk using a Struers Accutom precision cutting machine. The parts were cleaned using a Branson 2210 MT ultrasonic cleaner. The parts were cleaned before and after the cutting operation for 5 minutes each in a bath of ethanol solution. An example of the manufactured part and the cut away designed porosities can be found in Figure 4.

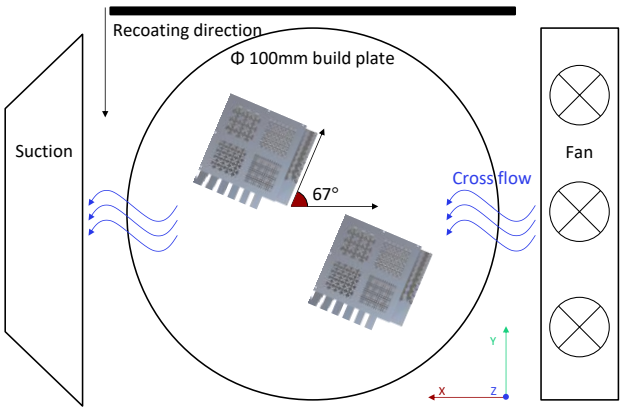

Figure 2 Build layout for manufacturing benchmark parts

2.4. Characterization

The designed porosities were characterized by X-ray computed tomography (XCT). XCT scanning was carried out using a Nikon XT H 225 at the 3D Imaging center at DTU. The parts were scanned with a voxel size of 16.288 µm. The software Avizo® by Thermo Fisher Scientific was used to carry out the analysis of scanned data. The simplified workflow for characterization is illustrated in Figure 3.

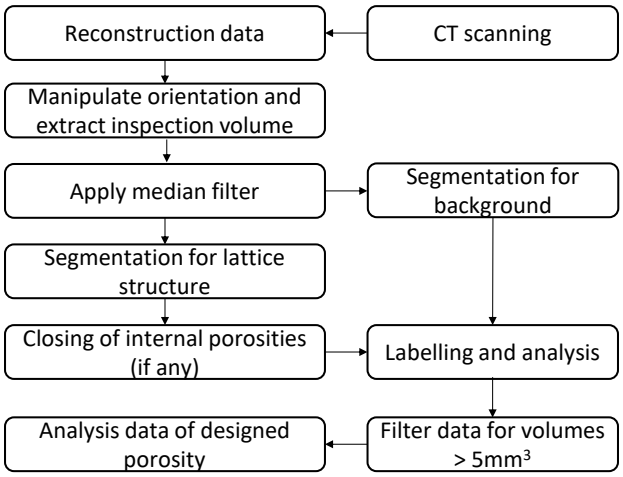

Figure 3 Workflow for XCT characterization

A similar process of data reconstruction was followed to obtain binarized slices of the designed porosities. The slicing plane was normal to the struts of the lattice structure, so as to obtain their cross-section for dimensional characterisation. Three central binarized image slices were used for characterising the strut diameter. A simple MATLAB code for strut identification and extracting the diameter by fitting a circle was used.

3. Results

The parts were successfully manufactured at the different duty cycles of 70%, 80%, 90 %, and 100% respectively. The designed porosities were cut away and scanned using the XCT.

By means of XCT scanning and image analysis, a visualisation of the designed porosities in the manufactured parts is displayed in Figure 5. Since the designed porosity samples were cut out of the main benchmark part the XCT-scanned bulk volumes don't look similar. However, the area of interest, the designed porosity was unaffected by the sample preparation.

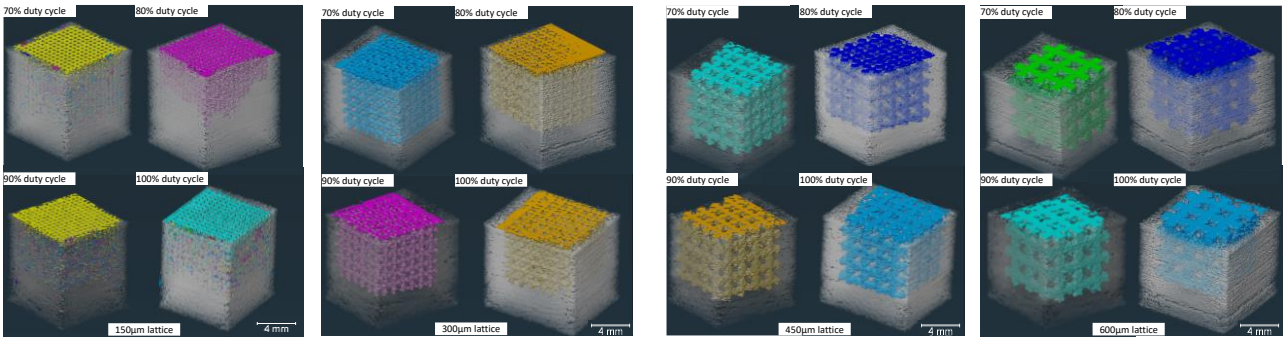

Figure 5 XCT of designed porosities manufactured with different lattice dimensions at various duty cycles

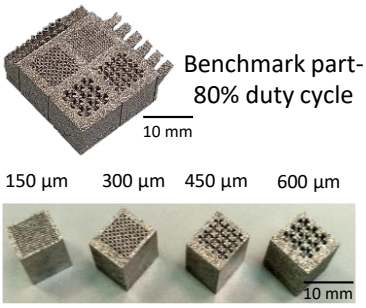

Figure 4 Part manufactured with 80% duty cycle

The visualizations in Figure 5 provide a good indication of the extent to which micro-features can be resolved on the current L-PBF system using pulsed and continuous wave lasers. In Figure 5 looking at the visualisation for the porosities designed with a 150µm lattice strut, it is observed that they were not manufactured as per expectations. Multiple small porosities were created instead of a singular interconnected porosity. However, the part manufactured at an 80% duty cycle had interconnected porosity but not for the entirety of the designed volume. The lack of interconnected porosity could possibly be due to multiple factors with the underlying issue being the melting/sintering of powders adjacent to the laser scanning region.

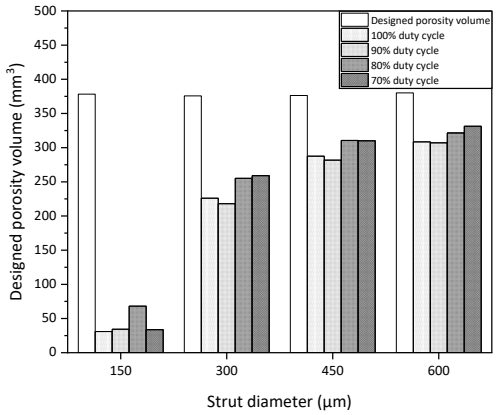

Figure 6 Comparison of designed porosities

The accuracy of the designed porosities was analysed by comparing the volume of the interconnected porosities (as per design) to the manufactured interconnected porosity (seen in the visualizations). The results from the analysis were plotted in a bar graph as seen in Figure 6. The graphical results indicate that the volume of the manufactured porosities were not the same as that of the designed porosities. However, the manufactured porosity volumes were closest to the designed porosity for the largest lattice and furthest away for the smallest lattice. The results indicate that the accuracy of the manufactured porosity decreases along with a decrease in the lattice size. The results don't indicate a linear increase in the manufactured volume with an increase in pulsing. However, if the results from the porosities manufactured with 70% & 80% are considered as similar and the ones manufactured with 90% & 100% are considered as similar then a clear improvement is observed in accuracy. There is a possibility that the pulsing duty cycles are closely spaced hence the chance of major improvements were not observed. Probably higher frequencies and lower duty cycles should have also been considered while planning the current body of work.

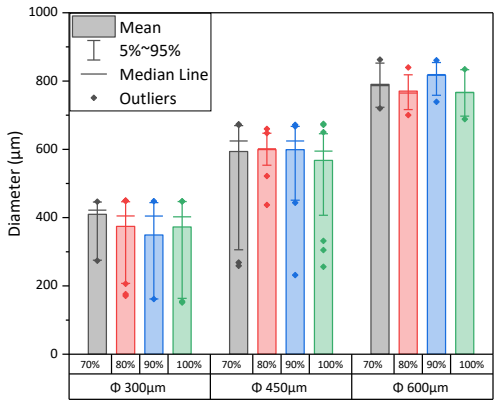

Figure 7 Strut diameter characterization

The dimensions of the struts of lattices used for the designed porosities are presented in Figure 1. The diameter for smallest strut of 150µm was not characterized since the cross sectional image slices didn't provide sufficient information for the code to identify the struts (circles). Results from the remaining designed porosities indicate that the manufactured struts are not of the designed diameters. They have been manufactured at diameters larger than the intended geometry, with the variance decreasing as the strut diameter increases. The measurements for struts of diameter 600µm show signs of a normal distribution implying that for those designed porosities the struts are well defined. However, for the small strut sizes, not as much, with the struts of diameter 300µm being less defined and non-homogeneous in dimensions. It should be noted that the method of characterization is not precise as it is based of 3 cross sectional images only. And the code used fits a circle whereas extracting an equivalent diameter or ellipse fitting might provide more information for better analysis.

4. Discussion

Even though the manufacture of designed porosity with the finest lattice dimensions was unsuccessful, it provided a good understanding of the capability of BAXTER. This knowledge helps design parts with features better suited for the L-PBF system,

keeping the smallest manufacturable feature size in mind. The sintering/melting of adjacent powders could be an outcome of the small unit cell, i.e. 600µm. In that case, per layer, the linear spacing between the laser scanning zones was only 300µm. It has been observed in previous research that shorter scan lines can lead to heat accumulation[11]. Like 'Skywriting' (which is a common feature on new commercial scanner systems), research indicates that scanning strategies considering melt pool formation and growth can help reduce heat accumulation from short-line scans [12]. A possible solution to achieve near-designed porosity would be by using a single exposure strategy, i.e. exposing the laser at points instead along vectors in fine feature regions. Based on the strut diameter results, there is an indication that the open architecture BAXTER L-PBF system and the systems controller GLAMS should also be investigated for precision operation. At the time of this work, the system didn't allow for 'Skywriting'. The scan speed used is much lower than that used in commercial systems and hence improvements on that front can provide better results in a following investigation.

Previous work from N. Taniguchi et al [13], shows that the % porosity and pore size plays an important role in designing for biomedical implants, since porosity allows for vascularisation which leads to good bone ingrowth in the implant. They show that pores sized from 300µm to 600µm, show good bone in-growth over 8 weeks. Hence highlighting the role of the porosity volume in biomedical applications. The current work shows another way to manufacture and characterize the % porosity of parts designed with the intent for biomedical applications.

Pulsing of the laser showed an improvement in the accuracy of the designed porosity volume. However, analysis in this work was limited to using a comparison of the interconnected porosity volume and hence more characterizations are required to understand the complete outcome of pulsing the laser for designed porosities. The current work is lacking information about the mechanical response and biological response of designed porosities made using PW L-PBF which will be considered for future investigations. Also, surface characterization of the features and porosity analysis of the struts will help provide a better understanding designed porosities. The samples were XCT scanned with a voxel size of 16.288µm, hence the available dataset can be used in the future to analyse the strut dimensions and surface. On the other hand, the porosity of the strut would require another XCT scan at a higher resolution or a different method of characterization.

The learnings from the show that pulsing and scanning strategies need to be optimized for the manufacture of designed porosities. But pulsing can already be implemented in the manufacture of parts (mm range) which require tight tolerances.

5. Conclusion

This work shows that designed porosities (upto a feature size of 300µm) can be successfully built on the open architecture system BAXTER with and without pulsing. The parts with designed porosities were characterized using XCT and successfully analysed by means of the produced void volume. This work, therefore, provides a way of characterizing and validating designed porosities (of any kind) in the future using XCT. The interconnected porosity volumes were closest to designed values for the lowest 70% duty cycle (high pulse duration) as compared to the highest 100% duty cycle (no pulse). Hence the manufactured porosities prove the basic hypothesis that PW L-PBF performs better than CW L-PBF.

For future work, an experimental study on the melt pool behaviour for PW L-PBF will be carried out on BAXTER to develop an understanding of its effect on the manufacture of micro-features and features with overhanging structures. The upgradation of the AM Lab software to incorporate multiple and new scanning strategies will be carried out, to make the most of the future work. The primary purpose of manufacturing designed porosities was for the future possibility to apply this technology to make biomedical implants. Hence, the next iteration of this manufacturing designed porosities will be planned such that they can be checked for their response to biological assays, corrosion testing and compressive testing.

References

[1] R. K. Chen, Y. an Jin, J. Wensman, and A. Shih, "Additive manufacturing of custom orthoses and prostheses-A review," *Addit Manuf*, vol. **12**, pp. 77–89, 2016, doi: 10.1016/j.addma.2016.04.002.

[2] A. G. Demir, P. Colombo, and B. Previtali, "From pulsed to continuous wave emission in SLM with contemporary fiber laser sources: effect of temporal and spatial pulse overlap in part quality," *International Journal of Advanced Manufacturing Technology*, vol. **91**, no. 5–8, pp. 2701–2714, 2017, doi: 10.1007/s00170-016-9948-7.

[3] S. Weiner and H. D. Wagner, "The material bone: Structure-mechanical function relations," *Annual Review of Materials Science*, vol. **28**, no. 1, pp. 271–298, 1998, doi: 10.1146/annurev.matsci.28.1.271.

[4] S. Ponader *et al.*, "In vivo performance of selective electron beam-melted Ti-6Al-4V structures," *J Biomed Mater Res A*, vol. **92**, no. 1, pp. 56–62, 2010, doi: 10.1002/jbm.a.32337.

[5] B. Vandenbroucke and J. P. Kruth, "Selective laser melting of biocompatible metals for rapid manufacturing of medical parts," *Rapid Prototyp J*, vol. **13**, no. 4, pp. 196–203, 2007, doi: 10.1108/13552540710776142.

[6] A. Charles, M. Bayat, A. Elkaseer, L. Thijs, J. H. Hattel, and S. Scholz, "Elucidation of dross formation in laser powder bed fusion at down-facing surfaces: Phenomenon-oriented multiphysics simulation and experimental validation," *Addit Manuf*, vol. **50**, 2022, doi: 10.1016/j.addma.2021.102551.

[7] D. Thomas, "The Development of Design Rules for Selective Laser Melting The Development of Design Rules for Selective Laser Melting," University of Wales Institute, Cardiff, 2010.

[8] S. A. Andersen, "Open Architecture Laser Power Bed Additive Manufacturing," Technical University of Denmark, 2020. [Online]. Available: https://orbit.dtu.dk/en/publications/open-architecture-laser-power-bed-additive-manufacturing

[9] S. A. Andersen, K. A. Meinert, M. B. Kjer, V. K. Nadimpalli, and D. B. Pedersen, "A Unified System Controller for Open-Source Powder Bed Fusion Systems," in *Proceedings of the 33rd Annual International Solid Freeform Fabrication (SFF) Symposium*, 2022, pp. 1273–1285.

[10] E. H. Valente, V. K. Nadimpalli, S. A. Andersen, D. B. Pedersen, T. L. Christiansen, and M. A. J. Somers, "Influence of atmosphere on microstructure and nitrogen content in AISI 316L fabricated by laser-based powder bed fusion," in *European Society for Precision Engineering and Nanotechnology, Conference Proceedings - 19th International Conference and Exhibition, EUSPEN 2019*, 2019, pp. 244–247. Accessed: Jun. 16, 2023. [Online]. Available: www.euspen.eu

[11] Z. Li, R. Xu, Z. Zhang, and I. Kucukkoc, "The influence of scan length on fabricating thin-walled components in selective laser melting," *Int J Mach Tools Manuf*, vol. **126**, pp. 1–12, 2018, doi: 10.1016/j.ijmachtools.2017.11.012.

[12] Y. Liu *et al.*, "An optimized scanning strategy to mitigate excessive heat accumulation caused by short scanning lines in laser powder bed fusion process," *Addit Manuf*, vol. **60**, pp. 2214–8604, 2022, doi: 10.1016/j.addma.2022.103256.

[13] Taniguchi, N., Fujibayashi, S., Takemoto, M., Sasaki, K., & Otsuki, B. (2016). Effect of pore size on bone ingrowth into porous titanium implants fabricated by additive manufacturing : An in vivo experiment. *Materials Science & Engineering C*, **59**, 690–701, doi: 10.1016/j.msec.2015.10.069